

EXPERIMENTAL IDENTIFICATION ON A GEAR WHINE NOISE IN THE AXLE SYSTEM OF A PASSENGER VAN

S. J. KIM¹⁾ and S. K. LEE^{1)*}

¹⁾Department of Mechanical Engineering, Inha University, Incheon 402-751, Korea

(Received 11 August 2006; Revised 2 January 2007)

ABSTRACT—This paper presents practical work on the reduction of gear whine noise. In order to identify the source of the gear whine noise, transfer paths are searched and analyzed by operational deflection shape analysis and experimental modal analysis. It was found that gear whine noise has an air-borne noise path instead of structure-borne noise path. The main sources of air-borne noise were the two global modes caused by the resonance of an axle system. These modes created a vibro-acoustic noise problem. Vibro-acoustic noise can be reduced by controlling the vibration of the noise source. The vibration of noise source is controlled by the modification of structure to avoid the resonance or to reduce the excitation force. In the study, the excitation force of the axle system is attenuated by changing the tooth profile of the hypoid gear. The modification of the tooth profile yields a reduction of transmission error, which is correlated to the gear whine noise. Finally, whine noise is reduced by 10 dBA.

KEY WORDS : SUV car, Gear, Whine, Axle, Passenger van, Operational deflection shape analysis, Vibro-acoustic

1. INTRODUCTION

In today's highly competitive automotive industry, the vehicle sound quality becomes more and more important (Lee *et al.*, 1993, 2003; Lee 1995, 2001, Becker and Yu, 1999a, 1999b; Ko *et al.*, 2006). There is a constant pressure to achieve a low vehicle interior noise level in system design, especially for a passenger van. For an axle system, gear whine noise is one of the major factors in achieving the vehicle interior sound quality. This paper presents the results of the practical research to reduce the whine noise of an axle system of a passenger van. The problem occurs in the compartment of a passenger van. In general, gear whine noise has two paths: airborne and structure-borne (Sun *et al.*, 2003, 2004). In order to identify the transfer path of whine noise, the accelerations on all transfer paths from the axle to the car body are measured together with interior noise of the passenger van simultaneously. From vibration tests, it is found that the isolator between the body and axle system can reduce enough the vibration transfer energy from the axle system to the car body. Therefore, the structure-borne noise is not significantly important for whine noise. As the next process, operational deflection shape analysis and experimental modal analysis are used to identify the source of airborne noise due to the structural behavior of the axle system during acceleration of the passenger van. It is

found that the major reason for airborne noise is the vibro-acoustic noise of the axle system. This vibro-acoustic noise is controlled by reducing the excitation force due to gear meshing. The excitation force is reduced by modifying the tooth profile, which is related to the transmission error. Transmission error is very much correlated with gear whine noise (Donley *et al.*, 1992; Glover and Rauhen, 2003; Tarutani and Maki, 2000; Athavale *et al.*, 2001; Houser and Harianto, 2001). In the paper, the transmission error of the ring gear has been reduced by modification of the tooth profile of the ring gear under test. Finally, whine noise in the compartment of the passenger van is reduced by 10 dBA. The sound quality due to whine noise is also improved.

2. MEASUREMENT OF INTERIOR NOISE

An axle system with a gear ratio of 3.616 is developed. The number of teeth of a pinion gear is 13 and the number of teeth of a ring gear is 47 in an axle system. A passenger van loaded with this axle system is accelerated in order to have a subjective evaluation of gear whine noise. During acceleration, the gear whine noise in the compartment of the passenger van is especially heard at 60 km/h and 120 km/h. To identify the source of this whine noise objectively, first, the interior noise is measured at the front seat. Figure 1 shows the waterfall map for the noise signal. On this waterfall map, two peaks are clearly identified at 1,800 rpm and 2,300 rpm as shown in

*Corresponding author. e-mail: sangkwon@inha.ac.kr

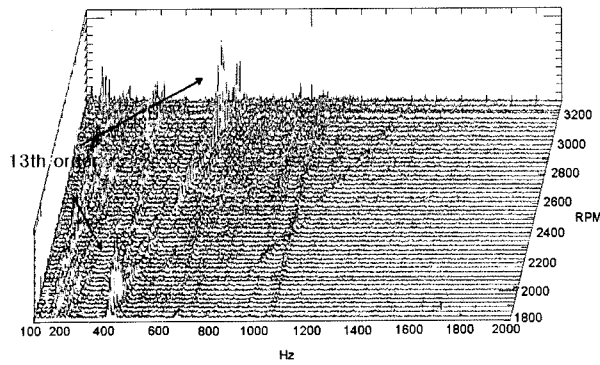


Figure 1. Waterfall map for the interior noise data.

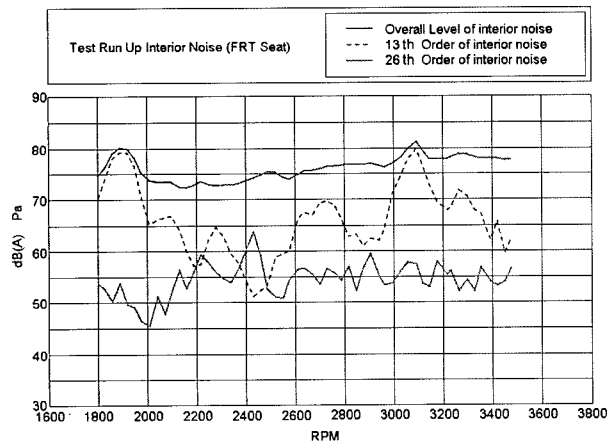


Figure 2. Order analysis for interior noise.

Figure 2. These two peaks occur at the frequency band, which is the meshing frequency of the hypoid gear of the axle system. These peaks well correspond with the previous subjective evaluation. Meshing frequency of the hypoid gear is 13 times the rotation speed of driveshaft since the number of teeth of a pinion gear is 13. In Figure 2, it infers that gear whine noise is related to the harmonics of the meshing frequency of hypoid gear in an axle system.

3. IDENTIFICATION OF TRANSFER PATH

Gear whine noise originates from the excitation force by the meshing of a hypoid gear as shown in Figure 3. There are two paths for whine noise: structure-borne noise path and airborne path. The transfer of the vibration energy from the axle system to car body induces structure-borne noise. The direct transfer of vibro-acoustic sound due to the shell vibration of an axle system from axle system to compartment of a car induces air-borne noise.

3.1. Structure-borne Path

The structural vibration of an axle system is measured at several points as shown in Figure 4. Three accelerations

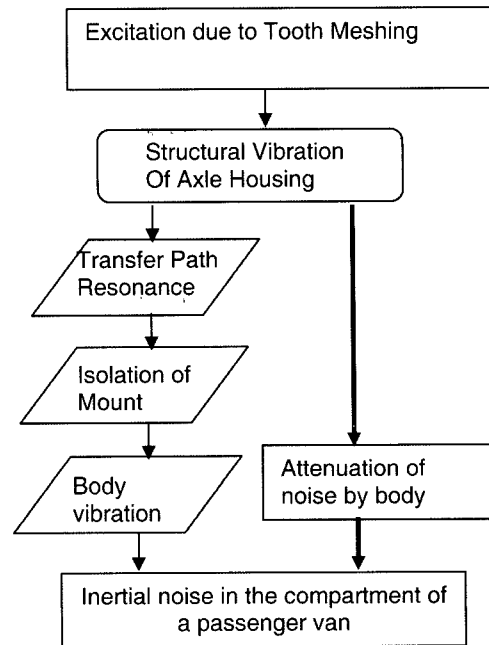


Figure 3. Transfer paths of air-borne noise and structure-borne for gear whine noise in an axle system; — : Structure-borne path, — — : air-borne path.

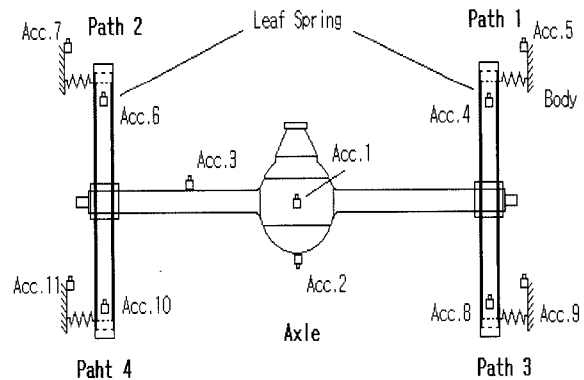


Figure 4. Measurement point of the structure vibration of an axle system (Acc. means the points measured by accelerometer).

are measured on the housing of axle and eight accelerations are measured on the bracket of isolation system during acceleration from 1,800 rpm to 3,500 rpm of driveshaft speed. Figure 5 shows the photo information about the attachment of three accelerometers attached on the axle housing.

Figures 6, 7 and 8 show the waterfall map for the vibration data measured at the point 1, 2, and 3 of axle system respectively. From these results, there is one structure resonance around 3,100 rpm. Resonance frequency is about 670 Hz ($3,100 \text{ rpm} \times 13/60$). The other resonance

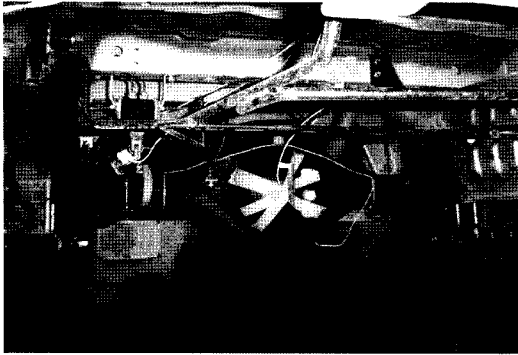


Figure 5. Photo explanation for measurement point of the structure vibration of an axle system.

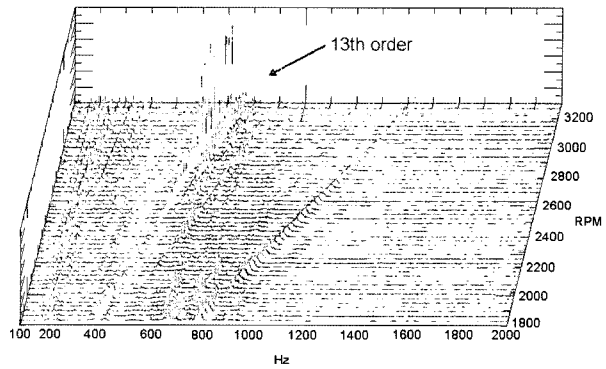


Figure 8. Waterfall map for the vibration data measured at the point 3 of axle housing.

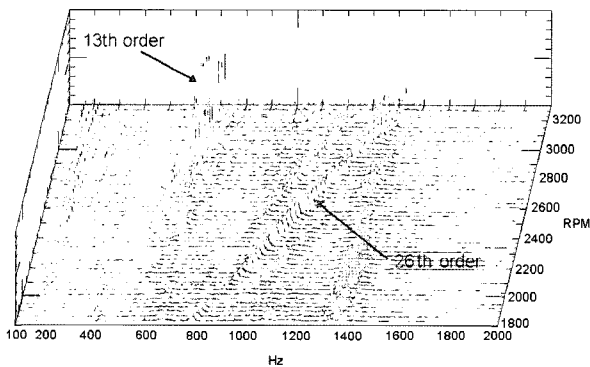


Figure 6. Waterfall map for the vibration data measured at the point 1 of axle housing.

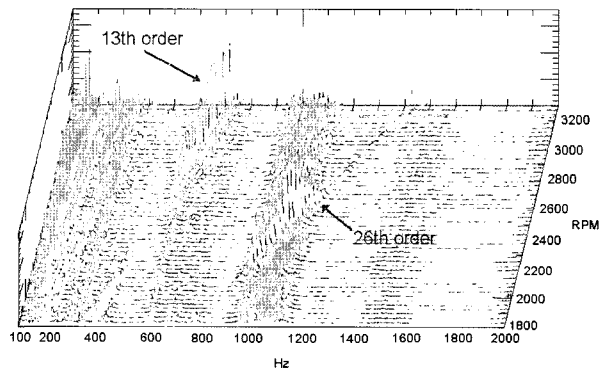


Figure 9. Waterfall map for the vibration data measured at the point 4 before isolation rubber.

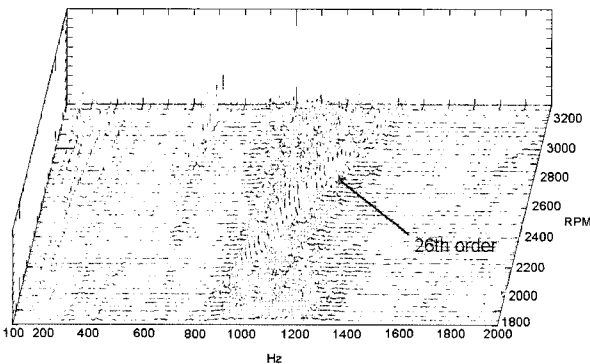


Figure 7. Waterfall map for the vibration data measured at the point 2 of axle housing.

of house structure occurs at 2,600 rpm. Resonance frequency is about 1,100 Hz ($2,600 \text{ rpm} \times 26 / 60$). Two peaks caused by resonance are clear in Figure 6 and Figure 7, but in Figure 8 only one peak is clear caused by 13th order of driveshaft speed.

Points 1 and 2 are the places on the hypoid gear housing. Point 3 is the place of the axle system. Therefore, at 670 Hz, the resonance caused by 13th order of drive-

shaft speed is global mode of axle system. At 1,100 Hz, the resonance caused by 26th order of driveshaft speed is the local mode of axle housing itself. This local mode does not contribute to the interior since there is no gear whine noise at 1,100 Hz as shown in Figure 1. The global mode excites the whole axle system. Therefore, the axle system has high vibration level at all other four points (point 4, 6, 8 and 10 in Figure 4) before the isolator as shown in Figure 4. It is confirmed with vibration result measured at point 4 as shown in Figure 9.

The isolator, which is installed between the axle system and the car body, attenuates this horrible vibration due to global mode of the axle system. Figure 10 shows the waterfall map for the vibration data measured at point 5. This point is the place after the isolator rubber; there is no resonance peak. Although there are a few resonances in the axle system, all vibration energy is dissipated through damping of the rubber isolator, which is installed between the axle system and the car body. Therefore, the gear whine noise as shown in Figure 1 is not caused by structure-borne noise. Finally, Figure 11 shows the set-up of the measurement equipment for noise and vibration testing for a passenger van.

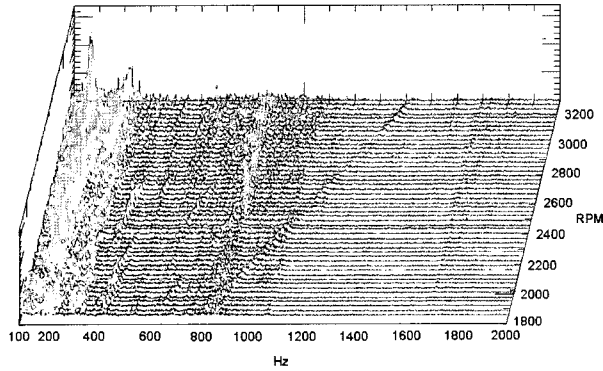


Figure 10. Waterfall map for the vibration data measured at the point 5 after isolation rubber.

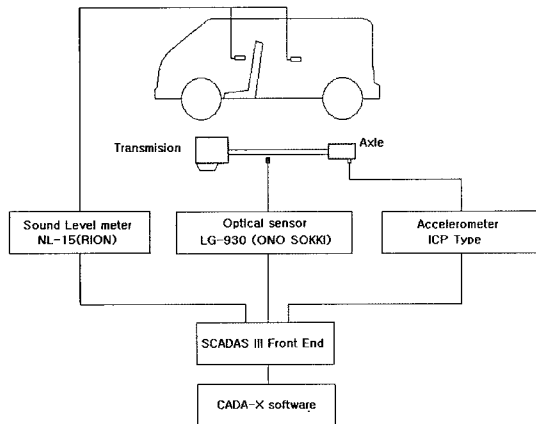


Figure 11. Set-up of measurement equipment for noise and vibration test for a passenger van.

3.2. Modal Analysis and Operational Deflection Shape Analysis

Although the two resonances existing in the axle system do not affect the gear whine noise inside of the car throughout structural vibration-transmission, they can affect the gear whine noise as the air-borne sound. In order to identify the structure mode, experimental modal analysis and operational deflection shape analysis are used. operational deflection shape analysis (ODSA) can be obtained by using phase difference between reference point X and moving point Y. The governing equation is given by (Wyckaert and Van der Auweraer, 1995),

$$\phi_i = Y_i \cdot \frac{X^*}{|X|} = B \cdot e^{j(b-a)} \quad (1)$$

where

$$\begin{aligned} X &= A \cdot e^{ja} \\ Y &= B \cdot e^{ja} \end{aligned} \quad (2)$$

Figure 12 shows the measurement point for operational deflection shape analysis and experimental modal ana-

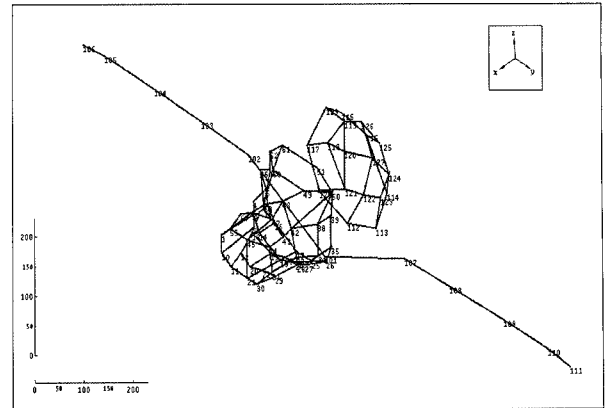


Figure 12. Measurement point for operational deflection shape analysis and experimental modal analysis.

lysis. The number of points is 125. At these 125 points, vibration is measured during acceleration from 1,800 rpm to 3,200 rpm of driveshaft. The phase difference for each point as shown in Figure 12 is calculated by using Equation (1).

Operational deflection shapes are obtained and plotted in Figure 13. There are three major operational deflection shape analysis. Two are global modes and the other one is a local mode. One global mode is a torsional mode as shown in Figure 13(a), the other a global mode is the bending mode as shown in Figure 13(b). The local mode is the bulge mode of the axle housing as shown in Figure 3(c). The torsional mode of the axle system occurred at 1,800 rpm with 13th order of drive shaft and its frequency is 433 Hz. It affects gear whine noise and the air-borne noise. The bending mode of the axle system occurred at 3,100 rpm with 13th order of drive shaft and its frequency is 670 Hz. It affects gear whine noise and the air-borne noise. The bulge mode of the axle housing occurred at 2,600 rpm with 26th order of drive shaft and its frequency is 1,100 Hz. It does not affect the gear whine noise as much as the two global modes as shown In Figure 1, since it is a local mode and vibration energy is not enough to radiate the sound. Major three modes appearing in the operational deflection shape analysis in Figure 13 are confirmed with experimental modal analysis. Experimental set-up for modal analysis is arranged as shown in Figure 14. The number of excitation points is the same point as points as shown in Figure 12. In order to identify the major modes of the axle system, the sum of transfer functions measured at the 125 points as shown in Figure 12 is calculated and plotted in Figure 15.

In this figure, two peaks at low frequency around 115 Hz and 300 Hz are found and one peak is identified around 900 Hz. The first two peaks are global modes: torsional mode and bending mode. The last one is the bulge mode of the axle housing, which is a local mode as

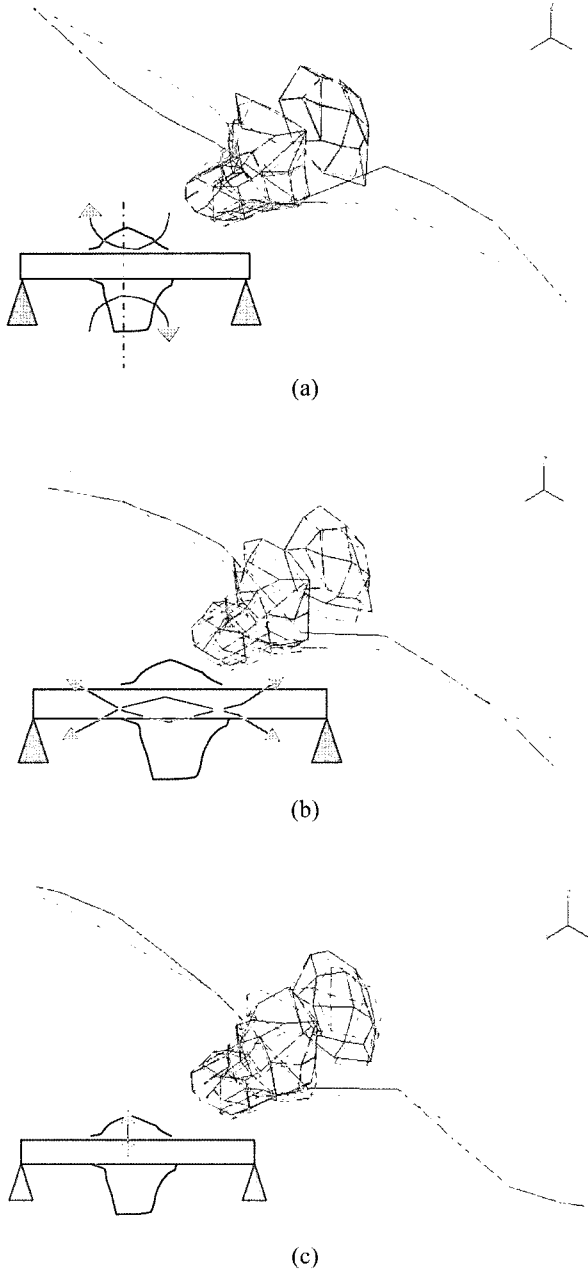
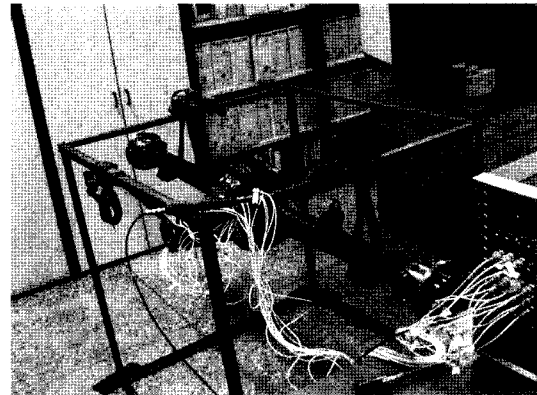
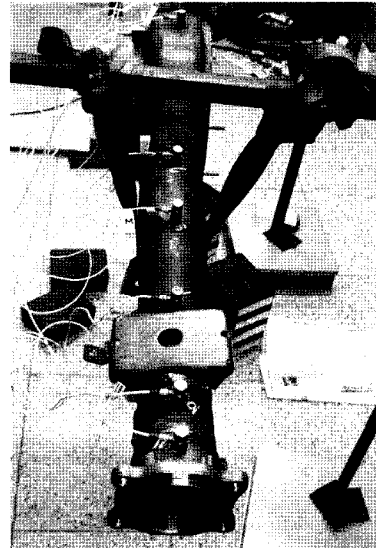


Figure 13. operational deflection shape analysis during acceleration from 1,800 rpm to 3,200 rpm of driveshaft.

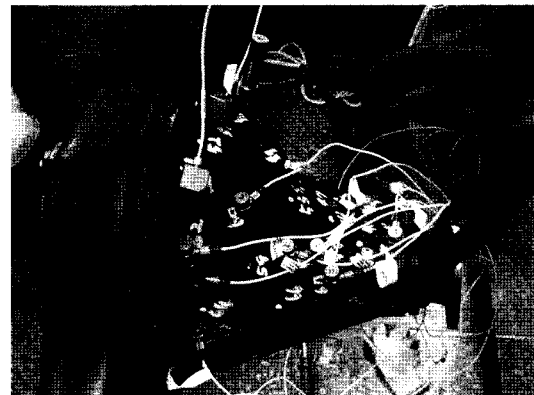
shown in Figure 16. The natural frequency of each mode is shifted down to low frequency compared with the frequency obtained from the operational deflection shape analysis as shown in Figure 13, because the boundary condition of the structures between operational deflection shape analysis and experimental modal analysis is different. For operational deflection shape analysis, the axle system is installed on the car. Therefore the structure is



(a)



(b)



(c)

Figure 14. Photo illustration for experimental modal analysis of axle system.

constrained by the suspension system of a real car. For experimental modal analysis, the axle system under test is installed freely on the frame as shown in Figure 14.

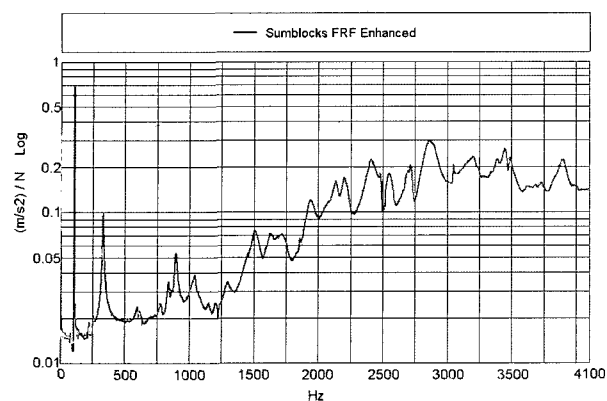


Figure 15. Sum of transfer functions measured at the 125 points.

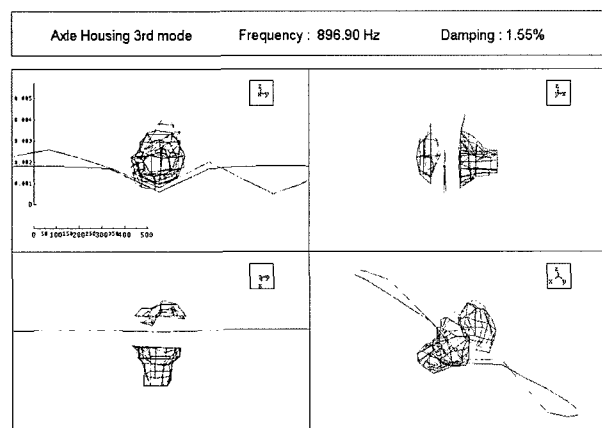


Figure 16. Mode shape for 3rd mode (bulge of axle housing) of the axle system.

Therefore, there is a frequency difference between the resonance frequency obtained operational deflection shape analysis and that obtained experimental modal analysis.

4. DESIGN MODIFICATION OF AXLE

In the previous section it was found that structure-borne noise does not contribute to gear whine noise because all vibrational energy caused by the resonance of the axle system is damped out through the isolator between the body and the axle system. Therefore, it is inferred that part of the vibration energy caused by resonance of the axle system is radiated as vibro-acoustic energy. This vibro-acoustic energy is air-borne noise and a major source for gear whine noise in the compartment of a passenger van. There are three methods for reducing this air-borne noise. The first is a design modification of the car body with high acoustic transmission loss required. The second is a structure modification of the axle system to avoid resonance. The last one is to attenuate the ex-

Table 1. The profile of tooth in the ring gear.

	Cutter Dia.	Tooth Profile	Contact Area
Original	22.9 cm	Slow	
Modification	19.1 cm	Steep	

Table 2. The design details of the ring gear.

	Cutting by 9 inch cutter	Cutting by 7.5 inch cutter
Tooth profile	Helix form	Helix form
Cutting method	Gleason	Gleason
Cutter diameter	22.9 cm	19.1 cm
Module	5.268	4.907
Number of teeth	47	47
Face width	31.75	31.75
Shaft angle	90°	90°
Pinion offset	38.10	38.10
Spiral angle	26°49'	22°5'
Whole depth	9.83	10.57
Addendum	1.13	1.78
Dedendum	8.70	8.79
Face angle	76°12'	76°2'
Root angle	74°9'	69°53'
Pitch angle	79°21'	75°
Gear ratio	4.89R (44X9)	4.89R (44X9)
Mating gear	3009 4580	3009 4580
Backlash	0.15~0.20	0.13~0.20
Transmission error	0.104	0.056

citation force by modifying the profile of the teeth in the hypoid gear. For economical efficiency, in the paper, the last method is adapted for the reduction of whine noise.

4.1. Modification of Tooth Profile

According to previous research results (Sun *et al.*, 2003; Donley *et al.*, 1992; Glover and Rauen, 2003; Tarutani and Maki, 2000; Athavale *et al.*, 2001; Houser and Harianto, 2001) and the company experience, transmission error is correlated to the gear whine noise. In the paper, the tooth profile is modified from a flat form to bent form listed in Table 1.

In order to modify the tooth profile, the original ring gear is processed by using a 22.9 cm cutter, but the modified ring gear is processed by using a 19.1 cm cutter. In the contact area, the black area is the initial contact area of teeth. The outline is the contact area of teeth under full load condition. The design details of the ring gear under test are listed in Table 2.

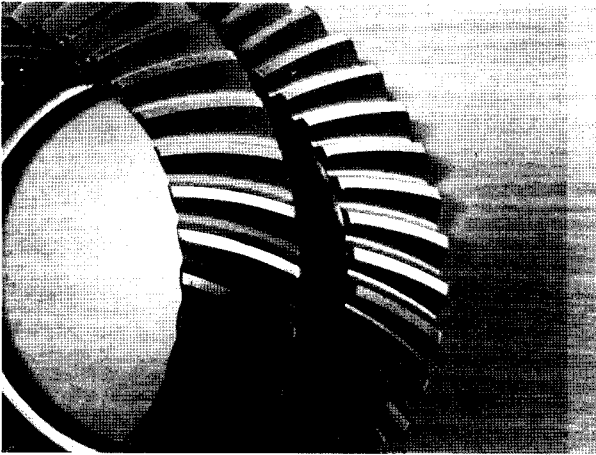


Figure 17. Photo of two ring gears of axle system.

4.2. Transmission Error

Gleason 500 Ht is used for the measurement of transmission error of two-ring gears. The total transmission error is reduced from 0.104 to 0.056 as listed in Table 2. According to Table 1, the initial contact area of two gears has the same area. However, the contact area of the ring gear with high transmission error goes out of the boundary of tooth face under full-load condition while the contact area of the ring gear with low transmission error is inside of the boundary of the tooth face. Figure 17 shows a photo of two ring gears. The upper one shows the ring gear with high transmission error; the bottom one shows the ring gear with low transmission error.

4.3. Gear Whine Noise Reduction

The modified axle system with new profile tooth is replaced of noisy axle system and installed on the passenger van under test. Interior noise for a passenger van is measured and its results are plotted in Figures 18 and 19.

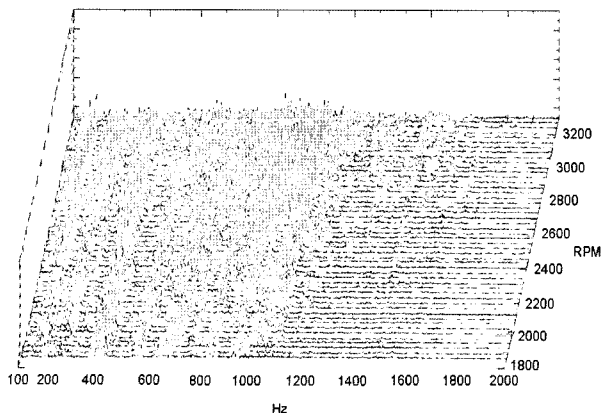


Figure 18. Waterfall map for interior noise of a passenger van with modified axle system.

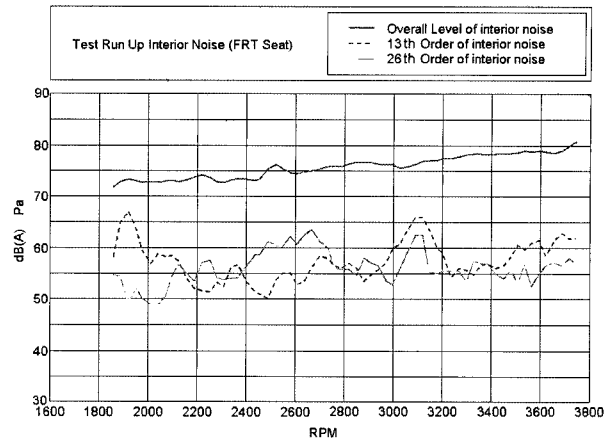


Figure 19. Order analysis for interior noise of a passenger van with modified axle system.

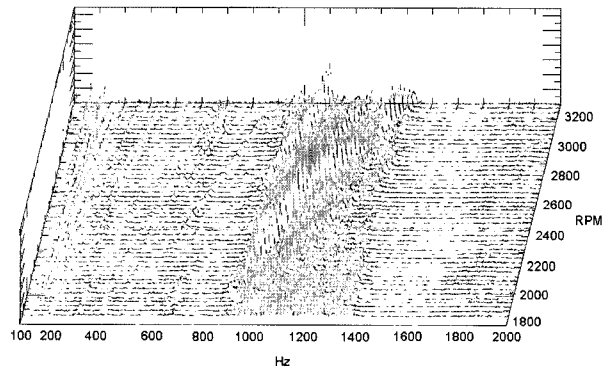


Figure 20. Waterfall map for structure vibration of a axle housing measured on the positing 2 in modified axle system.

Vibration on the axle housing at point 2 is also measured. Figure 20 shows results of the vibration test. From these results, high vibration around 1,800 rpm and 3,200 rpm of driveshaft speed, as shown in Figure 7, is removed since the excitation force due to tooth meshing is significantly attenuated by reducing transmission error although structure resonance exists. Therefore, Interior noise also reduced up to 10dB(A) at the same speed of driveshaft speed as shown in Figure 18 and 19 comparing with Figure 1 and 2. Around 2,600 rpm of driveshaft speed, the 26th order component of vibration is still high level since it is a local mode of axle housing and it does not significantly contribute to the gear whine noise.

5. CONCLUSIONS

Basic noise and vibration tests for a passenger van are assessed for the identification of problems. Gear whine noise occurs around 1,800, which is the speed of drive shaft, and 3,200 rpm, at which vibration level is also

high.

Experimental modal analysis and operational deflection shapes are used to identify the vibration transfer path. It is found that two global modes contribute to the resonance of an axle system around 1,800 rpm and 3,200 rpm. The former is the torsion mode of axle system around 433 Hz; the latter is bending mode of axle system around 603 Hz. Vibrations caused by these modes are attenuated through an isolator at the mount point of the axle system. Therefore, it is inferred that the structure-borne noise is not contributing to gear whine noise. However these modes contribute to the air-borne noise for gear whine noise.

In order to control the air-borne noise, the structure should be modified to avoid resonance or the excitation force should be reduced. For gear whine noise, the modification of structure mode requires very high stiffness in structure. In the paper, instead of modification of the axle system, the excitation force is attenuated by reducing the transmission error by optimizing the profile of teeth of the axle gear.

By reinstalling the new axle system with optimized tooth profile on the same passenger van with gear whine noise problem, interior noise is reduced by 10 dBA.

ACKNOWLEDGMENTS—This work was supported by Automobile Component Base Technology Project. This work was also partly supported by DYMOS Company in Korea.

REFERENCES

- Athavale, S., Krishnaswami, R. and Kuo, E. (2001). Estimation of statistical distribution of composite manufactured transmission error, a precursor to gear whine for a helical planetary gear system. *SAE Paper No.* 2001-01-1507.
- Becker, S. B. and Yu, S. (1999). Objective noise rating of gear whine. *SAE Paper No.* 1999-01-1720.
- Becker, S. B. and Yu, S. (1999). Gear noise rating prediction based on objective measurement. *SAE Paper No.* 1999-01-1721.
- Donley, M. G., Lim T. C. and Steyer, G. C. (1992). Dynamic analysis of automotive gearing systems. *J. Passenger Cars: Mechanical Systems* **101**, **6**, 958–968.
- Glover, R. and Rauen, D. (2003). Gear transmission error for use with ger inspection machine. *SAE Paper No.* 2003-01-1663.
- Houser, R. and Harianto, J. (2001). Manufacturing robustness analysis of noise excitation and design of alternative gear sets. *SAE Paper No.* 2001-01-1417.
- Ko, K. H., Kook, H. H. and Heo, S. J. (2006). New technique in the use of vibro-acoustical reciprocity with application to the noise transfer function measurement. *Int. J. Automotive Technology* **7**, **2**, 173–177.
- Lee, S. K., Yeo, S. D. and Choi, B. U. (1993). Identification of the relation between crankshaft bending and interior noise of A/T vehicle in idle state. *SAE Paper No.* 930618.
- Lee, S. K. (1995). Weight reduction and noise refinement of hyundai 1.5 liter powertrain. *SAE Paper No.* 940995.
- Lee, S. K. (2001). Vibrational power flow and its application to a passenger car for identification of vibration transmission path. *SAE Paper No.* 2001-01-1451.
- Lee, S. K., Chae, H. C., Park, D. C. and Jung, S. G. (2003). Booming index development for sound quality evaluation of a passenger car. *SAE Paper No.* 2003-01-1497.
- Sun, Z., Voight, M. and Steyer, G. (2004). Driveshaft design guidelines for optimized axle gear mesh NVH performance. *FISITA 2004*, F20004V287, Seoul, Korea.
- Sun, Z., Steyer, G., Meinhardt, G. and Ranek, R. (2003). NVH robustness design of axle System. *SAE Paper No.* 2003-01-1492.
- Tarutani, I. and Maki, H. (2000). A new tooth flank form to reduce transmission error of helical gear. *SAE Paper No.* 2000-01-1153.
- Wyckaert, K. and Van der Auweraer, H. (1995). Operational analysis, transfer path analysis, modal analysis: Tools to understand road noise problems in cars. *SAE Paper No.* 951752.